Available online at www.sciencedirect.com

SciVerse ScienceDirect

Ceramics International 38 (2012) 3397–3402

CERAMICS INTERNATIONAL

www.elsevier.com/locate/ceramint

Optical characteristics of Er^{3+}-doped PMN–PT transparent ceramics

Zhihao Wei [a], Yanlin Huang [a,*], Taiju Tsuboi [b], Yosuke Nakai [b], Jiangtao Zeng [c], Guorong Li [c,**]

[a] College of Chemistry, Chemical Engineering and Materials Science, Soochow University, Suzhou 215123, China
[b] Faculty of Engineering, Kyoto Sangyo University, Kamigamo, Kyoto 603-8555, Japan
[c] Shanghai Institute of Ceramics, Chinese Academy of Sciences, Shanghai 200050, China

Received 24 November 2011; received in revised form 19 December 2011; accepted 19 December 2011
Available online 27 December 2011

Abstract

The pure and Er^{3+}-doped (0.5, 1.0, 2.0 and 5.0 mol.%) PMN–0.25PT transparent ceramics were fabricated. The phase formations were investigated by X-ray diffraction patterns. The optical transmittance and absorption spectra were measured. The Er^{3+}-doping in the region of 0.5–2.0 mol.% can enhance the optical transmittance of Er^{3+}-doped PMN–0.25PT transparent ceramics. The Er^{3+} doping can modify the optical absorption near the band gap energy of PMN–0.25PT. The shift of the absorption edge to higher energy was observed in the case of the low doping concentration (<2.0 mol.%) and the red-shift was found for the higher doping concentration (5.0 mol.%). This has been explained by the combined effects of ion polarization and localized defect energy level. The direct energy gaps, the indirect energy gaps and phonon energy contributing in the indirect transition were determined based on the theory of band to band transitions.

Keywords: Transparent ceramic; PMN–PT; Optical materials and properties

1. Introduction

$Pb(Mg_{1/3}Nb_{2/3})O_3$ (PMN) with perovskite-structure is known as the best representative of relaxor ferroelectrics [1]. Another perovskite-structure ferroelectric $PbTiO_3$ (PT) has been also paid attention because of various applications such as actuators, capacitors, transducers, and micro-electromechanical systems [2–4].

Mixed PMN and PT, $(1-x)Pb(Mg_{1/3}Nb_{2/3})O_3$–$xPbTiO_3$ (PMN–PT or PMN–xPT), where x means the mixing ratio, have been also widely investigated from its large piezoelectric and electrostrictive responses to applied electric field in single crystals, bulk ceramics, and thick films [5]. PMN–PT materials are suitable for applications in multilayer capacitors, actuators, sensors, and electro-optical devices because the high dielectric permittivity, high piezoelectric properties, and high electrostriction [6]. Giant piezoelectric response has been observed in a morphotropic phase boundary (MPB) composition at about $x = 0.35$ [7–9]. The influence of rare earth ions (RE) doping on the phase transition behavior, and relaxor ferroelectrics of PMN–PT have been widely have been reported [10].

In addition, PMN–PTs are the most promising nonlinear optical materials because of its extremely high electro-optic (EO) coefficient and strong photorefractive effect [11–13]. Uchino [14] has reported that quadratic EO coefficient of 0.88PMN–0.12PT (22×10^{-16} $(m/v)^2$) is twice as large as that of PLZT ((Pb,La)(Zr,Ti)O_3) ($R = 9 \times 10^{-16}$ $(m/v)^2$). Jiang et al. [15] reported that EO coefficient of PMN–PT could reach to a value of 28×10^{-16} $(m/v)^2$. PMN–PT and ferroelectric oxide materials doped with RE ions have been also studied for optical amplification and laser [15,16]. Recently, Ruan et al. [17,18] reported the excellent EO properties of La^{3+}-doped PMN–PT x/75/25 (which means La^{3+} concentration of $x = 2$, 3, 4 at.% with PMN/PT ratio of 75–25) transparent ceramics. Its Kerr constant is higher than 60×10^{-16} $(m/v)^2$, which was reported the highest among the well-known relaxor ferroelectric systems [18]. It is necessary to study the modification of RE ions doping on the optical properties of PMN–PT transparent ceramics because this transparent host material has excellent specialties, e.g., good optical clarity, high optical damage threshold, and large EO effect. This will be useful for application to electro-optics devices.

* Corresponding author. Tel.: +86 13584875529; fax: +86 512 65880089.
** Corresponding author. Tel.: +86 21 52412990; fax: +86 21 52413903.
E-mail addresses: huang@suda.edu.cn, huangyanlin@hotmail.com (Y. Huang), grli@mail.sic.ac.cn (G. Li).

0272-8842/$36.00
doi:10.1016/j.ceramint.2011.12.051

In the present paper, the un-doped and 0.5, 1.0, 2.0 and 5.0 mol.% Er^{3+}-doped PMN–0.25PT transparent ceramics were fabricated. The crystal phases were checked by X-ray diffraction patterns. The Er^{3+}-doping in PMN–0.25PT transparent ceramics is expected to modify the optical transmittance near the band gap energy. The shifts behavior of the absorption edge at different Er^{3+} doping levels has been discussed by the combined effects of ion polarization and localized defect energy level.Experiments

The transparent ceramics of un-doped Er^{3+}-doped (0.5, 1.0, 2.0, 5.0 mol.%) $Pb(Mg_{1/3}Nb_{2/3})O_3$–$0.25PbTiO_3$ (PMN–0.25PT) were fabricated by a two-stage sintering method as described by Ruan et al. [17]. The starting materials in Ruan's method to fabricate PMN–PT transparent ceramics are PbO, MgO, Nb_2O_5 and TiO_2. They sintered the samples at a temperature $\geq$1000 °C for more than 8 h under hot-pressing of 50–100 MPa. The difference in this experiment from Ruan's method is that $4(MgCO_3)\cdot Mg(OH)_2\cdot 5H_2O$ was used as the precursor material instead of MgO. The major advantages of this method are that the pressure (20–80 MPa) is decreased and the sintering time (6–8 h) is shortened.

Firstly, the mixtures of $4(MgCO_3)\cdot Mg(OH)_2\cdot 5H_2O$ and Nb_2O_5 were ball-milled for 2 h. The slurry was dried and preheated at 1000 °C for 4 h. Secondly, PbO (excess of 5–10% for liquid-phase sintering) and TiO_2 were added into the powders obtained in the first step. The mixtures were ball-milled for 24 h. The slurry was dried again and heated at 950 °C for 2 h and then uniaxially pressed into pellets. Thirdly, the pellet was sintered in an oxygen atmosphere at 950–1000 °C, and then hot-pressed at 1100–1200 °C for 6–8 h at pressure of 20–80 MPa. Disk specimens of 17 mm in diameter and 15 mm in thickness, to be used for measuring the optical absorption, were mirror polished on both surfaces.

The XRD pattern was collected on a Rigaku D/Max-2000 diffractometer operating at 40 kV, 30 mA with Bragg–Brentano geometry by using Cu Kα radiation (λ = 1.5418 Å). The optical transmittance and absorption were measured by a Shimadzu UV-3100 UV–VIS–NIR spectrophotometer. The experiments were performed at room temperature.Results and discussionFig. 1 shows the XRD patterns of PMN–0.25PT transparent ceramics doped with different concentrations of Er^{3+} ions (0.5, 1.0, 2.0, 5.0 mol.%). The crystal faces, e.g. [1 0 0], [1 1 0], [2 0 0], etc., exhibit sharp and symmetric single diffraction peaks with rhombohedral symmetry. The main crystal phase of all the Er^{3+}-doped PMN–0.25PT transparent ceramics is perovskite structure. However, in 5.0 mol.% Er^{3+}-doped PMN–0.25PT transparent ceramic, the presence of a peak [2 2 2] from pyrochlore phase as marked in Fig. 1 was observed, but the perovskite phase still keep more prominent. X-ray diffraction measurement was used to calculate the relative content of the perovskite phase, k_{perov} (in %), using an approximate equation:

$$k_{perov} = \frac{I_{perov} \times 100}{I_{perov} + I_{pyro}} \quad (1)$$

where I_{perov} and I_{pyro} were the integral intensity of the [1 1 0] perovskite diffraction peak and the [2 2 2] pyrochlore diffraction peak, respectively [19,20]. The relative content of the

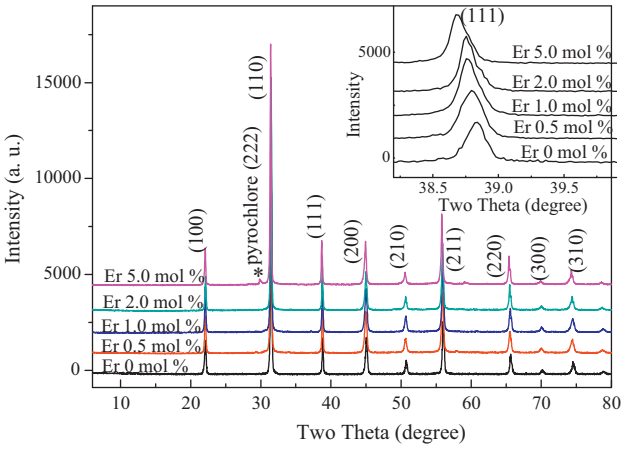

Fig. 1. XRD patterns of PMN–0.25PT transparent ceramics doped with different concentrations of Er^{3+} ions. Inset shows the enlargement of the partial XRD patterns.

pyrochlore phase in PMN–0.25PT:Er^{3+} 5.0 mol.% is about 2.0%. The replacement of Pb^{2+} by Er^{3+} might lead to the agglomeration of Pb^{2+} at the grain boundary, since the reaction activity between Pb^{2+} and Nb^{5+} is larger than that of Mg^{2+}, pyrochlore phase is easy to form. Zheng et al. [16] suggested that in Er^{3+}-doped PMN–PT thin films the outward diffusion of Nb^{5+} and the inward diffusion of Ti^{4+} could compensate Er^{3+} on the *B* site positions to achieve charge balancing. Consequently, Er-substitution results in Nb-rich and Nb-poor regions, and results in the second phase generation when a certain amount of Er^{3+} doping is achieved (0.5 mol.%). The Nb-rich regions are pyrochlore, whereas the Ti-rich regions remain perovskite. The results in Fig. 1 indicate that the maximum tolerated doping concentration in Er^{3+}-doped PMN–PT transparent ceramics (5.0 mol.%) is much higher than that of Er^{3+}-doped PMN–PT thin film (0.5 mol.%).

With increasing Er^{3+} doping, all the XRD peaks shift toward to the smaller diffraction angle (inset in Fig. 1), indicating that the lattice constants of Er^{3+}-doped samples become larger than those of un-doped one. The polycrystalline nature of PMN–PT transparent ceramics makes this material homogenous in structure, and thus polarization independent. This feature is especially convenient in devices design since there would not need to consider the crystal orientation that is usually troublesome in single crystal materials [15].

The transmittance spectra of un-doped and Er^{3+}-doped PMN–0.25PT transparent ceramics in UV–visible and IR region are shown in Fig. 2. The ceramics are all transparent in the visible and IR region. The samples become completely absorbing around 400 nm, indicating an optical absorption edge in near UV. This is similar to the PMN–PT single crystal [21] or the most oxygen-octahedral perovskites [22]. Since the refractive index is about 2.3 in infrared region and 2.44 at 633 nm, the reflection loss at the air/ceramic interface is estimated to be about 29%, which is similar to the value obtained in the La^{3+}-doped PMN–0.25PT transparent ceramic [17]. Except for the absorption by the material, the light losses are mainly caused by the scattering due to domain walls.

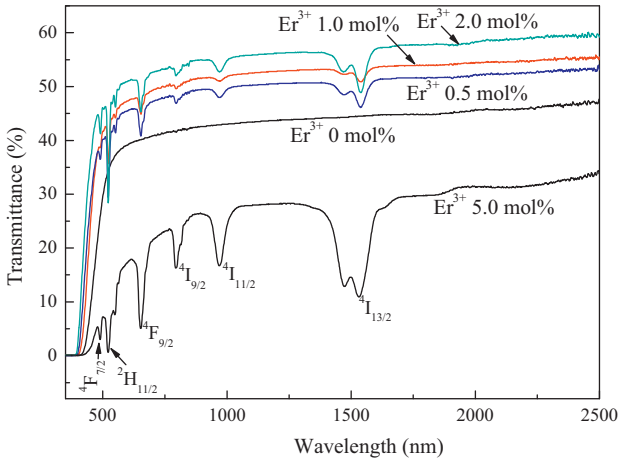

Fig. 2. The transmittance curves of the PMN–0.25PT transparent ceramics doped with different concentrations of Er^{3+} ions.

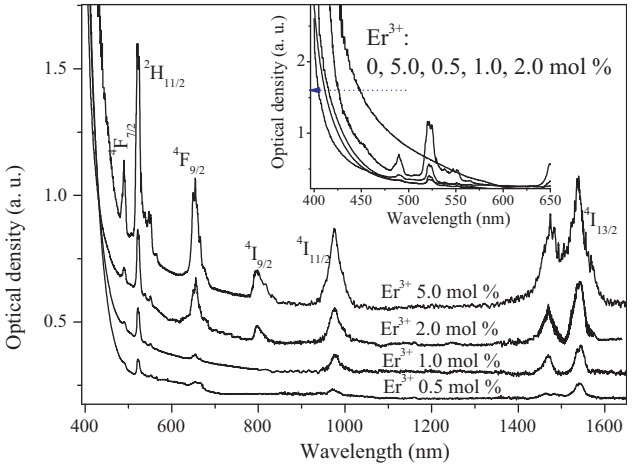

Fig. 4. The absorption spectra of Er^{3+} ions doped PMN–0.25PT transparent ceramics with thickness of 1.5 mm. To compare one spectrum with another, the absorption of PMN–0.25PT:Er^{3+} 1.0, 2.0, and 5.0 mol.% are shown by some up-shifts. Inset shows the enlarged absorption spectra in the region of near optical bang gap.

The transmittance of un-doped PMN–0.25PT in the visible region can be estimated to be 43.0%. The transmittance of PMN–0.25PT transparent ceramics with Er^{3+} doping levels of 0.5, 1.0 and 2.0 mol.% are 50%, 53%, and 57%, respectively. The absorption peaks from the ground state $^4I_{15/2}$ to the upper states can be clearly observed in the transmittance spectra of PMN–0.25PT:Er^{3+} transparent ceramics.

In comparison with the un-doped PMN–0.25PT, the increasing of Er^{3+} doping from 0.5 to 1.0 and 2.0 mol.% gradually enhances the transmittance. However, the transmittance is lower in the case of heavy Er^{3+} 5.0 mol.% doping (28.0%). This can be seen in the photographs of the un-doped and Er^{3+}-doped PMN–0.25PT transparent ceramics with various contents (0.5, 1.0, 2.0 and 5.0 mol.%) as in Fig. 3. Each pellet is about 17 mm in diameter and 1.5 mm thick. All the letters under the ceramics can be seen, however, the samples doped at different concentrations show different transparencies, which are in consistent with the transmittance spectra in Fig. 2.

In order to examine the optical band gap energy for the PMN–0.25PT:Er^{3+} transparent ceramics, the optical absorption spectra were recorded in the UV–visible and IR region. Fig. 4 shows the absorption spectra in the range from 200 to 1650 nm. It is well known that the main feature of the absorption edge of semiconductors, particularly at the lower values of the absorption coefficient, is an exponential increase of the absorption coefficient $\alpha(\nu)$ with photon energy $h\nu$ in accordance with an empirical relation [23]:

$$\alpha = \alpha_0 \exp\left(\frac{h\nu}{\Delta E}\right) \tag{2}$$

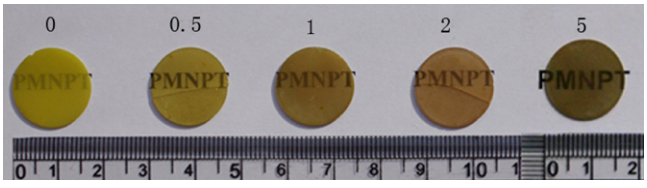

Fig. 3. The photos of Er^{3+}-doped PMN–0.25PT transparent ceramics (1.5 mm thick). The numbers in the photo are the Er^{3+} doping levels in mol.%.

where α_0 is a constant, ΔE is the Urbach energy and ν is the frequency of radiation. The absorption coefficient $\alpha(\nu)$ can be determined near the edge using the formula:

$$\alpha(\nu) = \frac{2.303 \times \mathrm{OD}}{H} \tag{3}$$

where OD is the optical density in Fig. 4, and H the thickness of the samples (cm).

On the absorption spectra in Fig. 4, the strong absorption bands can be seen near 500, 650, 1000, and 1500 nm, corresponding to the excited energy levels of Er^{3+}. The intensity of Er^{3+} absorption bands increases rise with increasing Er^{3+} concentration. It appeared that, even when the Er^{3+} doping reaches as much as 5.0 mol.%, there is no indication of saturation and appearance of new band.

In the un-doped PMN–0.25PT ceramic, the cut-off absorption edge is not so steep (inset in Fig. 4), i.e., there seems to have a broad absorption band at 2.883–2.254 eV (430–550 nm). This absorption band locates just near the absorption edge of PMN–PT so that it decreases the transmission in this region. However, for the Er^{3+}-doped PMN–0.25PT transparent ceramics, this absorption band apparently disappeared. This is consistent with the enhancement of optical transmittance in the case of Er^{3+} doping in Fig. 2.

This optical improvement can be interpreted by the assumptions that the some possible color centers in pure PMN–PT could disappear after the Er^{3+} doping. Usually it is unavoidable that the evaporation of PbO could take place during the growing process of crystals and ceramics with Pb-composition. The lead vacancies as negative charge centers induce the appearance of negative charge centers related to V_{Pb}'', which could be the origin of the absorption bands in visible wavelength region. As a matter of fact, the trivalent ions are considered as being able to replace the Pb^{2+} ions, which creates the positive charge center related to, e.g. $(Er^{3+}{}_{Pb})^{\bullet}$, which could inert the optical activity of V_{Pb}'' due to most

probable $[2Er^{3+}{}_{Pb})^{\bullet}–V_{Pb}{}'']$ complexes.The similar mechanism has been well approved in scintillating crystal $PbWO_4$. In general, there are obvious absorption bands with maxima peaking at 2.95–3.10 eV (400–420 nm) and 3.54 eV (350 nm) in the absorption edge of pure $PbWO_4$, which greatly decreases the transmission in these wavelength regions [24]. To date, the commonly accepted viewpoint is that the so-called 350- and 420-nm absorption bands are related to hole-centers connecting with V_{Pb}. However, the optical transmission can be significantly improved by doping with trivalent ions, such as La^{3+}, Y^{3+}, Gd^{3+} and Lu^{3+} [25]. These trivalent ions could compensate the Pb^{2+}-deficiency, thus reduce the densities of the Pb^{2+}-related defects. Han et al. [26] have investigated the dielectric relaxation spectra of La^{3+}-doped $PbWO_4$ and concluded that the observed polarization was most probably due to the creation of $[2(La^{3+}{}_{Pb})^{\bullet}–V_{Pb}{}'']$ dipole complexes.

In Fig. 4, in comparison with the un-doped sample, the blue shift of the optical absorption edges in PMN–0.25PT:Er^{3+} 0.5, 1.0, and 2.0 mol.% can be observed. For the 5.0 mol.% Er^{3+}-doped PMN–0.25PT, the optical absorption edge returns to the lower energy region, i.e., red-shift.

It is known that the fundamental optical transitions include the direct transition and the indirect transition. The fundamental interband transitions of the PMN–PT include both direct and indirect transitions [27] According to Fermi's golden rule the absorption due to the allowed direct transition at $h\nu \geq E_g$ is expressed as follows:

$$(\alpha h\nu) \propto (h\nu - E_{gd})^{1/2} \quad (4)$$

where α is the absorption coefficient, $h\nu$ is the incident photon energy, and E_{gd} is the allowed direct band gap.

In the indirect transition, the electron transit from the top of the valence band to the bottom of the conduction band with co-participation of photons and suitable phonons. The absorption is expressed as follows [28]:

$$(\alpha h\nu) \propto (h\nu - E_{gi} \pm E_p)^2 \quad (5)$$

where E_{gi} is the indirect energy gap, and E_p is the energy of the absorbed (+) or emitted (−) phonons. The plots of the $(\alpha h\nu)^2$ versus $h\nu$ for the un-doped and Er^{3+}-doped (0.5, 1.0, 2.0, and 5.0 mol.%) PMN–0.25PT transparent ceramics in the photo energy region from 2.0 to 3.0 eV are shown in Fig. 5. The indirect energy gaps were determined by extrapolating the linear portion of the curves to zero, which are listed in Table 1.

The dependences of $(\alpha h\nu)^{1/2}$ on $h\nu$ are show in Fig. 6. As an example of PMN–PT:Er^{3+} 2.0 mol.%, the values of

Table 1
The values of direct band-gap E_{gd}, indirect band gap E_{gi} and the energy of the phonon E_p for undoped and Er^{3+}-doped PMN–0.25PT transparent ceramics.

Doping levels	E_{gd} (eV)	E_{g1} (eV)	E_{g2} (eV)	E_p (cm^{-1})	E_{gi} (eV)
0 mol.%	2.85 ± 0.01	2.505	2.311	783 ± 10	2.408
0.5 mol.%	2.96 ± 0.01	2.623	2.428	785 ± 10	2.526
1.0 mol.%	2.99 ± 0.01	2.721	2.524	788 ± 10	2.622
2.0 mol.%	3.02 ± 0.01	2.783	2.588	785 ± 10	2.686
5.0 mol.%	2.91 ± 0.01	2.553	2.359	784 ± 10	2.456

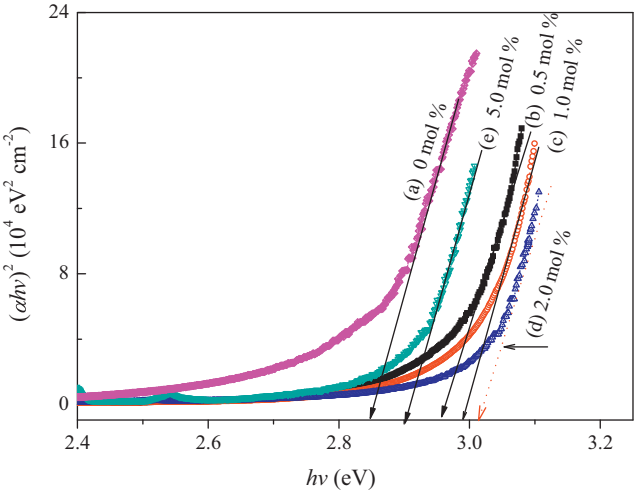

Fig. 5. The $(\alpha h\nu)^2$ versus photon energy ($h\nu$) of PMN–0.25PT:Er^{3+} transparent ceramics with thickness of 1.5 mm for the different Er^{3+} doping levels 0 mol.% (a), 0.5 mol.% (b), 1.0 mol.% (c), 2.0 mol.% (d), and 5.0 mol.% (e).

$E_{g1} = E_{gi} + E_p$ and $E_{g2} = E_{gi} - E_p$ were obtained to be $E_{g1} = 2.783$ eV and $E_{g2} = 2.5581$ eV by extrapolating the $(\alpha h\nu)^{1/2}$ versus $h\nu$ curve to zero. The indirect transition energy gap and the phonon energy could be determined as $E_{gi} = 1/2(E_{g1} + E_{g2}) = 2.686$ eV and $E_p = 1/2(E_{g1} - E_{g2}) = 0.0975$ eV (785 cm^{-1}), respectively. The values of phonon energy listed in Table 1 are similar to that of PMN–0.24PT single crystal (790 cm^{-1}) [27] or PMN–PT thin film (791.6 cm^{-1}) [13] recorded by Raman spectra.

The phonon around corresponding to the Nb–O–Mg bond stretching mode, which is sensitive to the distortion of the BO_6 octahedra (B = Ti, Nb, Mg), plays an important role in the indirect transition. It is found that the band gap energy (the indirect transition energy) of Er^{3+}-doped PMN–0.25PT decreases with increasing the Er^{3+} doping concentration from 0.5 mol.% to 2.0 mol.%. The decrease, however, stops when the concentration is 5.0 mol.%.

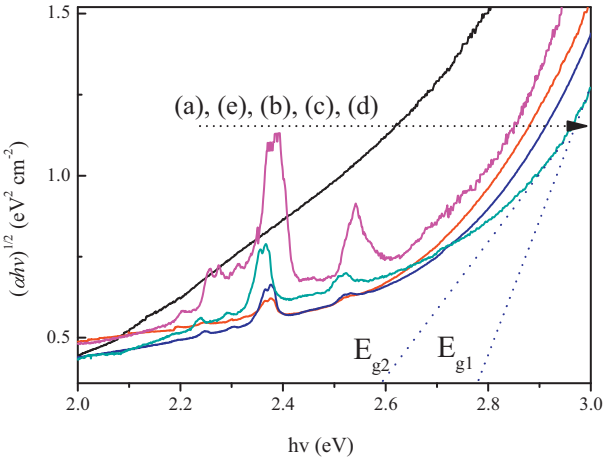

Fig. 6. The $(\alpha h\nu)^{1/2}$ versus photon energy ($h\nu$) PMN–0.25PT:Er^{3+} transparent ceramics with thickness of 1.5 mm for the different Er^{3+} doping levels 0 mol.% (a), 0.5 mol.% (b), 1.0 mol.% (c), 2.0 mol.% (d), and 5.0 mol.% (e).

In $A(B_1B_2)O_3$-type perovskite materials, the BO_6 (TiO_6, NbO_6, and MgO_6) octahedron building block determines the basic energy level. The *B*-cation *d* orbitals associated with its octahedron govern the lower lying conduction bands and while the *O*-anion 2*p* orbitals and its octahedron rule the upper valence bands. Other ions in the structure contribute to the higher-lying conduction band and have small effects. Furthermore, the $(B_1B_2)O_6$-octahedra structure has more significant effect on the optical properties of crystal than the *A*-site ions [22]. However, the doping of trivalent rare earth ions in PMN–PT could induce some disordering on the *A* sites, which can induce the changes of band gap absorption edge.

Like ABO_3-type and $(1-x)$PMN–*x*PT perovskite compounds $(1-x)$PMN–*x*PT has a common oxygen-octahedra structure that determines the basic energy level of the crystal [22,29]. The absorption edge of PMN–PT has been suggested to be caused by the transition from the O(2*p*) ground state to the *B*-site cation *d* orbits [21,27]. Therefore, the change of the distribution of the O^{2-} ion electron will directly affect the forbidden band gap.

The displacement of the indirect transition absorption edge of Er^{3+}-doped PMN–0.25PT transparent ceramics may be interpreted by using the ion-polarization model as follows. Science the polarizability of Er^{3+} is less than that of Pb^{2+}, the substitution of Er^{3+} into the Pb^{2+} sites in the PMN–PT lattice will give rise to decrease of the polarization of O^{2-} and thereby the energy of an electron transition from O(2*p*) ground state to the *B*-site cation *d* orbits will increase, leading to blue shift of the indirect transition absorption edge.

With increasing Er^{3+} doping level in PMN–0.25PT, the induced defects play an important role on the band gap absorption. Gupta et al. [30] have investigated the electrically induced strain and polarization studies of La^{3+} modified morphotropic phase boundary PMN–PT ceramics. It has been suggested that the charge unbalance due to La^{3+} substitution on the *A*-site was compensated by: (1) *B*-site vacancies, and (2) changing Mg/Nb/Ti ratio on the *B*-site. It has been found that non-stoichiometric ordering increases when La^{3+} is compensated by *B*-site vacancies (LaPMN–PT) and it decreases when La^{3+} is compensated by Mg/Nb/Ti (PLMN–PT).

On the other hand, with increasing the density of defects (or impurities), the band structure of PMN–PT is perturbed by the potential of the defects as well as by the localized strains induced by the defects. At high density the discrete energy levels of localized defect become a continual energy band. The defect energy bands tend to overlap with the conduction band and/or valence band of the PMN–PT, resulting in contraction of the optical gap.

4. Conclusions

The un-doped and 0.5, 1.0, 2.0 and 5.0 mol.% Er^{3+}-doped PMN–0.25PT transparent ceramics were fabricated. PMN–0.25PT:Er^{3+} 0.5, 1.0, 2.0, 5.0 mol.% transparent ceramics present perovskite structure. However, 5.0 mol.% Er^{3+}-doped PMN–PT transparent ceramic presents small pyrochlore impurity phase (below 2.0%). The Er^{3+}-doping in the concentrations of 0.5–2.0 mol.% can greatly enhance the transmittance, however, heavy Er^{3+}-doping, e.g., 5.0 mol.% deteriorates the transmittance. Er^{3+}-doping shows an obvious modification on the optical transmittance and absorption edge, which shows a violet-shift in the case of PMN–0.25PT:Er^{3+} 0.5, 1.0, and 2.0 mol.% compared to the un-doped sample. However, the absorption edges move toward lower energy when the Er^{3+} content is doped in 5.0 mol.%. The polarization effect may dominate with low values of Er^{3+} concentration (<2.0 mol.%), whose band gaps are broader than that of pure sample. However, the localized defect energy level effect dominates in heavily doped PMN–0.25PT transparent ceramic.

Acknowledgements

This work was supported by the Program of International Cooperation of the Chinese Academy of Sciences (Grant No. GJHZ1042) and the Priority Academic Program Development of Jiangsu Higher Education Institutions (PAPD) in China. The present work was also partially supported by the Grant-in-Aid for the Scientific Research from Kyoto Sangyo University in Japan.

References

[1] E.V. Colla, E.Y. Koroleva, N.M. Okuneva, Long-time relaxation of the dielectric response in lead magnoniobate, Phys. Rev. Lett. 9 (1995) 1681–1684.
[2] V.V. Shvartsman, A.L. Kholkin, C. Verdier, D.C. Lupascu, Fatigue-induced evolution of domain structure in ferroelectric lead zirconate titanate ceramics investigated by piezoresponse force microscopy, J. Appl. Phys. 98 (2005) 0941091–0941097.
[3] K.P. Chen, X.W. Zhang, X.Y. Zhao, H.S. Luo, Field-induced effect in the [1 1 1]-oriented $0.70Pb(Mg_{1/3}Nb_{2/3})O_3$–$0.30PbTiO_3$ single crystals, Mater. Lett. 60 (2006) 1634–1639.
[4] S. Zhang, R. Xia, L. Lebrun, D. Anderson, T.R. Shrout, Piezoelectric materials for high power, high temperature applications, Mater. Lett. 59 (2005) 3471–3475.
[5] H. Uršič, M.S. Zarnik, M. Kosec, $Pb(Mg_{1/3}Nb_{2/3})O_3$–$PbTiO_3$ (PMN–PT) material for actuator applications, Smart Mater. Res. 2011 (2011) 452901–452906.
[6] S.E. Park, T.R. Shrout, Ultrahigh strain and piezoelectric behavior in relaxor based ferroelectric single crystals, J. Appl. Phys. 82 (1997) 1804–1811.
[7] Z.G. Ye, M. Dong, Morphotrophic domain structures and phase transitions in relaxor-based piezo-ferroelectric $(1-x)Pb(Mg_{1/3}Nb_{2/3}O_3$–$xPbTiO_3)$ single crystals, J. Appl. Phys. 87 (2000) 2312–2319.
[8] D. Viehland, M.C. Kim, Z. Xu, J.F. Li, Long-time present tweedlike precursors and paraelectric clusters in ferroelectrics containing strong quenched randomness, Appl. Phys. Lett. 67 (1995) 2471–2473.
[9] J. Jiang, S.G. Hur, S.G. Yoon, Electrical properties of epitaxial $0.65Pb(Mg_{1/3}Nb_{2/3})O_3$–$0.35PbTiO_3$ thin films grown on buffered Si substrates by pulsed laser deposition, Int. J. Appl. Ceram. Technol. 8 (2011) 1393–1399.
[10] M. Kuwabara, S. Takahashi, K. Goda, K. Oshima, K. Watanabe, Continuity in phase transition behavior between normal and diffuse phase transitions in complex perovskite compounds, Jpn. J. Appl. Phys. 31 (1992) 3241–3244.
[11] Y.H. Lu, J.J. Zheng, M.C. Golomb, F.L. Wang, H. Jiang, J. Zhao, In-plane electro-optic anisotropy of $(1-x)Pb(Mg_{1/3}Nb_{2/3})O_3$–$xPbTiO_3$ thin films grown on (1 0 0)-cut $LaAlO_3$, Appl. Phys. Lett. 74 (1999) 3764–3766.
[12] K.Y. Chan, W.S. Tsang, C.L. Mak, K.H. Wong, Optical studies of $0.65PbMg_{1/3}Nb_{2/3}O_3$–$0.35PbTiO_3$ thin films, J. Eur. Ceram. Soc. 25 (2005) 2313–2317.

[13] X.L. Tong, K. Lin, D.J. Lv, M.H. Yang, Z.X. Liu, D.S. Zhang, Optical properties of PMN–PT thin films prepared using pulsed laser deposition, Appl. Surf. Sci. 255 (2009) 7995–7998.
[14] K. Uchino, Electro-optic ceramics and their display applications, Ceram. Int. 21 (1995) 309–315.
[15] H. Jiang, Y.K. Zou, Q. Chen, K.K. Li, R. Zhang, Y. Wang, H. Ming, Z.Q. Zheng, Transparent electro-optic ceramics and devices, Proc. SPIE 5644 (2005) 380–394.
[16] J. Zheng, Y. Lu, X. Chen, C.G. Mark, J. Zhao, Photoluminescence in erbium-doped $Pb(Mg_{1/3}Nb_{2/3})O_3$–$PbTiO_3$ thin films, Appl. Phys. Lett. 75 (1999) 3470–3472.
[17] W. Ruan, G.R. Li, J.T. Zeng, J.J. Bian, L.S. Kamzina, H.R. Zeng, L.Y. Zheng, A.L. Ding, Large electro-optic effect in La-doped $0.75Pb(Mg_{1/3}Nb_{2/3})O_3$–$0.25PbTiO_3$ transparent ceramic by two-stage sintering, J. Am. Ceram. Soc. 93 (2010) 2128–2131.
[18] W. Ruan, G.R. Li, J.T. Zeng, L.S. Kamzina, H.R. Zeng, K.Y. Zhao, L.Y. Zheng, A.L. Ding, Origin of the giant electro-optic Kerr effect in La-doped 75PMN–25PT transparent ceramics, J. Appl. Phys. 110 (2011) 0741091–0741097.
[19] B.J. Fang, C.L. Ding, J. Wu, Q.B. Du, J.N. Din, Effects of dopants on the synthesis of $Pb(Mg_{1/3}Nb_{2/3})O_3$–$PbTiO_3$ ceramics by the reaction-sintering method, Phys. Status Solidi A 208 (2011) 1641–1645.
[20] R.M.V. Rao, A. Halliyal, A.M. Umarji, Perovskite phase formation in the relaxor system $[Pb(Fe_{1/2}Nb_{1/2})O_3]_{1-x}$–$[Pb(An_{1/3}Nb_{2/3})O_3]_x$, J. Am. Ceram. Soc. 79 (1996) 257–260.
[21] X.M. Wana, X.Y. Zhao, H.L.W. Chan, C.L. Choy, H.S. Luo, Crystal orientation dependence of the optical bandgap of $(1-x)Pb(Mg_{1/3}Nb_{2/3})O_{3-x}PbTiO_3$ single crystals, Mater. Chem. Phys. 92 (2005) 123–127.
[22] Y.H. Bing, R. Guo, A.S. Bhalla, Optical properties of relaxor ferroelectric crystal: $Pb(Zn_{1/3}Nb_{2/3})O_{3-4.5\%}PbTiO_3$, Ferroelectrics 242 (2000) 1–11.
[23] M.A. Hassan, C.A. Hogarth, A study of the structural, electrical and optical properties of copper tellurium oxide glasses, J. Mater. Sci. 23 (1988) 2500–2504.
[24] M. Nikl, K. Nitsch, S. Baccaro, A. Cecilia, M. Montecchi, B. Borgia, I. Dafinei, M. Demoz, M. Martini, E. Rosetta, G. Spinolo, A. Vedda, M. Kobayashi, M. Ishii, Y. Usuki, O. Jarolimek, P. Reiche, Radiation induced formation of color centers in $PbWO_4$ single crystals, J. Appl. Phys. 82 (1997) 5758–5762.
[25] M. Kobayashi, Y. Usuki, M. Ishii, N. Senguttuvan, K. Tanji, M. Chiba, K. Hara, H. Takano, M. Nikl, P. Bohacek, S. Baccaro, A. Cecilia, M. Diemoz, Significant improvement of $PbWO_4$ scintillating crystals by doping with trivalent ions, Nucl. Instrum. Method A 434 (1999) 412–423.
[26] B. Han, X. Feng, G. Hu, P. Wang, Z. Yin, Observation of dipole complexes in $PbWO_4$:La^{3+} single crystals, J. Appl. Phys. 84 (1998) 2831–2834.
[27] J.J. Zhu, W.W. Li, G.S. Xu, K. Jiang, Z.G. Hu, M. Zhu, J.H. Chu, Abnormal temperature dependence of interband electronic transitions in relaxor-based ferroelectric $(1-x)Pb(Mg_{1/3}Nb_{2/3})O_{3-x}PbTiO_3$ ($x = 0.24$ and 0.31) single crystals, Appl. Phys. Lett. 98 (2011) 0919131–0919133.
[28] A. El-Korashy, A.A. El-Fadl, Temperature dependence of the optical band gap of nearly perfect K_2ZnCl_4 single crystals in the ferroelectric phase, Physica B 271 (1999) 205–211.
[29] S. Nomura, H. Arima, F. Kojima, Quadratic electro-optic effect in the system $Pb(Zn_{1/3}Nb_{2/3})O_3PbTiO_3$, Jpn. J. Appl. Phys. 12 (1973) 531–535.
[30] S.M. Gupta, Z. Xu, D. Viehland, Development of high electrically induced strain and low hysteric loss compositions for actuators, Appl Ferroelectr. 1 (1996) 245–248.